Journal of Integrative Agriculture 2026, 25(2): 540–552

Available online at ScienceDirect

Journal of Integrative Agriculture



RESEARCH ARTICLE

Effects of land use type on soil organic carbon in different soil types

Shunjie Zhu[1, 5*], Liangliang Xu[1*], Chengzhong He[1, 2*], Yongxing Guo[3], Changqun Duan[1], Xin Jiang[2], Shiyu Li[1#], Hailong Yu[4#]

[1] *Yunnan Key Laboratory for Plateau Mountain Ecology and Restoration of Degraded Environments/School of Ecology and Environmental Science, Yunnan University, Kunming 650500, China*
[2] *Kunming General Survey of Natural Resources Center, China Geological Survey, Kunming 650100, China*
[3] *School of Mathematics, Hangzhou Normal University, Hangzhou 311121, China*
[4] *Command Center of Natural Resources Comprehensive Survey, China Geological Survey, Beijing 100055, China*
[5] *Institute of International Rivers and Eco-Security, Yunnan University, Kunming 650500, China*

Highlights

- Soil organic carbon (SOC) content in brown and yellow-brown soils exceed those in red, yellow and purple soils.
- Spring irrigation plays a crucial role in enhancing SOC in farmland.
- Proper water management facilitates farmland carbon emissions reduction and carbon sink enhancement.

Abstract

Soil organic carbon (SOC) dynamics significantly influence ecosystem carbon source-sink balance, particularly in agroecosystems. However, uncertainty remains regarding optimal land use types for maximizing farmland carbon storage across different soil types, and identifying effective land management practices for enhanced carbon accumulation is essential for reducing agricultural emissions and strengthening carbon sinks. This study examined SOC variations in eastern Yunnan's subtropical highlands (2,132 sites), analyzing topsoil (0–20 cm) across five land uses (dryland, irrigated land, forestland, grassland and plantation) of five soil types (red, yellow, yellow-brown, brown, purple). The investigation explored relationships between SOC and edaphic factors (26 elements) to determine SOC influencing factors. The study area demonstrated a mean SOC content of 27.78 g kg^{-1}, with distinct spatial heterogeneity characterized by lower values in the southwestern sector and higher concentrations in the northeastern region. Brown soils displayed the highest SOC content (P<0.05), followed by yellow-brown then red, yellow, and purple soils. Irrigation significantly enhanced SOC storage, particularly in brown soils where irrigated land contained 2.2-, 2.4-, and 1.6-times higher SOC than forestland, grassland, and dryland, respectively. Similar irrigation benefits occurred in purple, yellow, and yellow-brown soils, indicating moisture limitation as the primary SOC constraint. Notably, SOC exhibited strong positive correlations with nitrogen, sulfur, and selenium. Nitrogen fertilization demonstrated dual benefits: enhancing SOC sequestration and promoting Se enrichment in crops, potentially supporting specialty agriculture. Although land use impacts on SOC varied across soil types (P>0.05), irrigation consistently emerged as the optimal management for carbon sink enhancement. These findings suggest that targeted water management could effectively reduce farmland carbon emissions in moisture-limited subtropical highlands. Strategic nitrogen application offers co-benefits for soil fertility and selenium biofortification, providing practical pathways for climate-smart agriculture in similar ecoregions.

Keywords: soil organic carbon, soil type, land use type, carbon storage, agroecosystems

Received 23 April 2025; Received in revised form 26 July 2025; Accepted 29 August 2025; Available online 26 September 2025
[#]Correspondence Shiyu Li, E-mail: lisy@ynu.edu.cn; Hailong Yu, E-mail: yhailong@mail.cgs.gov.cn
[*] These authors contributed equally to this study.

© 2026 CAAS. Publishing services by Elsevier B.V. on behalf of KeAi Communications Co. Ltd. This is an open access article under the CC BY-NC-ND license (http://creativecommons.org/licenses/by-nc-nd/4.0/). Peer review under responsibility of Editorial Board of *Journal of Integrative Agriculture*.
doi: 10.1016/j.jia.2025.09.030

1. Introduction

Soil organic carbon (SOC) constitutes the largest and most dynamic terrestrial organic carbon pool, playing a crucial role in regulating global carbon cycles and mitigating climate change (Luo *et al.* 2023; Si *et al.* 2024). Its accumulation and stability directly influence the capacity of terrestrial ecosystems to sequester atmospheric CO_2, serving as a key indicator for ecosystem carbon sink functionality and climate change adaptation strategies (Nyaupane *et al.* 2024). Consequently, carbon stabilization — specifically, protecting the soil carbon pool and enhancing carbon sink function — has emerged as a research priority (Roe *et al.* 2021). Land utilization for human activities alters soil physical, chemical, and biological processes, thereby affecting SOC dynamics (Yu *et al.* 2015). Agricultural soil contributes significantly to reducing greenhouse gas emissions, enhancing carbon sink effects and mitigating climate change (Zhou *et al.* 2023). Cropland has received considerable attention for its substantial carbon sequestration potential, with its soil carbon pool significantly influencing global climate change (Raza *et al.* 2020). Cropland SOC is heavily influenced by human activities, representing 14.5% of the total organic carbon stock of 89.61 Mt C in China (Lal R 2004). However, distinct differences exist in the cumulative effects of different land use types on SOC: compared with cropland, natural forests and artificial forests can retain an additional 20–40% of SOC in the 0–30 cm soil layer through continuous litter input and root turnover (Don *et al.* 2011; Poeplau and Don 2015); after grazing prohibition or reseeding of degraded grasslands, the average annual increase of SOC can reach 0.6 Mg C ha^{-1}, which is comparable to the carbon sequestration rate of the conversion from cropland to forestland (Yang Y *et al.* 2022; Gao *et al.* 2025); rubber, oil palms and other plantations can also enhance SOC *via* deep root systems and residue return under intensive management, though the increase is regulated by tree age and fertilization regimes (Guillaume *et al.* 2018). These variations indicate that, beyond cropland, land use types such as forestland, grassland and plantation all demonstrate significant potential for SOC enhancement, and their carbon sequestration efficiency is jointly influenced by vegetation types, management measures and climatic conditions. Therefore, systematic comparison of SOC accumulation under different land use and management scenarios will provide a scientific foundation for developing regional low-carbon land use strategies.

SOC content demonstrates considerable variation across different soil types. In the surface layer (0–10 cm), yellow soil exhibits higher SOC content compared to red soil, while at 10–30 cm depth, red soil contains more SOC than yellow soil, suggesting that soil horizons significantly influence carbon distribution (Wen *et al.* 2018). Analysis of surface soil in the 0–20 cm layer reveals that SOC content follows a decreasing sequence: brown soil>lime soil>yellow-brown soil>yellow soil>red soil>purple soil (Chen F 2022). These studies indicate that carbon sequestration efficiency under identical land use patterns varies significantly across soil types. Consequently, incorporating the interaction between land use and soil types into regional carbon sink assessment frameworks is crucial for accurate quantification of how different land use types contribute to carbon accumulation in various soil types.

Land use types reflect both natural conditions and human activities, affecting SOC content through organic matter input and regulation of SOC accumulation and release rates (Yang Y H *et al.* 2022). Research has revealed substantial differences in active organic carbon content under various land use practices, particularly in the surface layer, though these differences diminish with increasing soil depth (Li *et al.* 2014). Agricultural practices across different land use types influence nutrient transformation and bioavailability, including SOC, N, and phosphorus (P) content (Ebabu *et al.* 2020). Land use practices also affect SOC binding to soil particles and minerals (particularly iron (Fe)/aluminum (Al) oxides), aggregate stability, and fundamental ecosystem functions (Udom and Ogunwole 2015). The SOC content varies among land use types due to changes in environment, ecosystem structure, and soil structure resulting from anthropogenic disturbances (Xiao *et al.* 2023). Studies indicate that SOC content in grassland is higher than in cropland at soil depths of 10–20 cm (Wiesmeier *et al.* 2012; Nuralykyzy *et al.* 2023). However, research has shown that cropland can contain higher SOC than grassland (Li *et al.* 2019), with some instances showing elevated SOC levels in grasslands compared to forestland (Yang Y H *et al.* 2022). In our research on South Changshan Island, the SOC content in 0–30 cm reservoir soil exceeded that of adjacent orchards (Wang *et al.* 2014). While land use types clearly influence SOC accumulation within identical soil types, empirical research data remain limited. Most studies focus on specific regions or individual soil types, with few comprehensive assessments of land-use impacts across broad edaphic gradients, limiting our understanding of land use effects on SOC dynamics.

The study area selected was Fuyuan County in Qujing City, situated in the subtropical highlands of eastern Yunnan Province, Southwest China. We measured SOC in topsoil and analyzed fundamental physicochemical properties, including particle size distribution, pH, and concentrations of 26 elements: aluminum (Al), arsenic (As), boron (B), calcium (Ca), cadmium (Cd), cobalt (Co), chromium (Cr), copper (Cu), fluorine (F), iron (Fe), mercury (Hg), iodine (I), potassium (K), magnesium (Mg), manganese (Mn), molybdenum (Mo), nitrogen (N), nickel (Ni), phosphorus (P), lead (Pb), sulfur (S), selenium (Se), silicon (Si), titanium (Ti), vanadium (V), and zinc (Zn). The research examined SOC variations across 2,132 sampling sites in the subtropical plateau of eastern Yunnan, analyzing five land-use types (dryland, irrigated land, forestland, grassland, plantation) within five distinct soil types (red, yellow, yellow-brown, brown, purple). This study aims to determine whether land use patterns differently affect carbon storage across soil types and to elucidate the underlying mechanisms. These findings provide science-based land management strategies and practical approaches for implementing low-carbon, climate-resilient agriculture.

2. Materials and methods

2.1. Overview of the study area

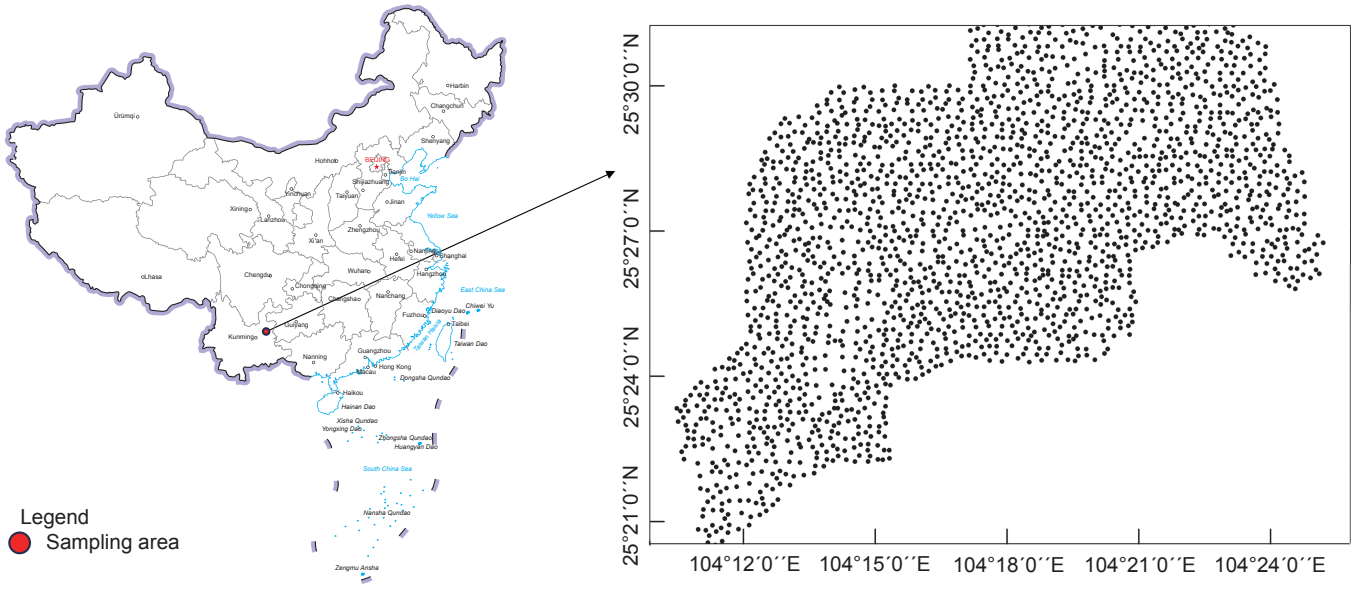
The study area is located in eastern Yunnan Province, China (104°10′–104°25′E, 25°21′–25°32′N), characterized by karst plateau–mountain topography with elevations ranging from 735 to 2,865 m. This subtropical climate zone has a mean annual temperature of 17.6°C (2011–2020), considerable sunshine duration, and mean annual precipitation of 974 mm (Fick and Hijmans 2017; Wang *et al.* 2017; Harris *et al.* 2020). Approximately 80% of precipitation occurs between May and October. Dryland agriculture constitutes the primary land cover, followed by forestland and grassland. Major crops include wheat (*Triticum aestivum*), maize (*Zea mays*), konjac (*Amorphophallus konjac*), and walnut (*Juglans regia*). The terrain exhibits a northwestward ascent and southeastward descent, featuring mountainous ridges and valleys.

2.2. Point layout and sample collection

A total of 2,132 topsoil sampling sites were established in 1 km^{-2} grids (Fig. 1), each subdivided into four 0.25 km^2 sampling cells. Each sampling cell contained an appropriate number of sampling points, primarily on agricultural land (sampling density, 8–11 points km^{-2}); all other land use types maintained a sampling density of 4–5 points km^{-2}. A total of 2,132 surface soil samples were collected from the study area, with a sampling density of 8.22 samples km^{-2}. The statistics of different land use patterns of various soil types at each sampling point in the study area are presented in Table 1.

The surface soil samples were collected in 2020 at a depth of 0–20 cm (each soil sample comprised sub-samples collected from a 0–20 cm soil column). A representative plot was selected for sampling, with the sampling point positioned at the plot center. Sub-samples were collected from the same plot as the initial field sample (maintaining the same plot type), at locations determined by the sampling plot shape. Distances from the global positioning system (GPS) location of the field sample to the sub-sampling points ranged from 20–50 m. Before sample collection, a bamboo shovel removed the soil surface portion that had direct contact with the hoe. The shovel was then used to dig downward along the sampling pit wall to a depth of 20 cm, extracting a cylindrical soil column (radius, 10 cm). The collected soil from each sample point was broken up, with root systems, straw, stones, insects, and other debris removed and placed in a bag. For each sample point, five sub-sample pit samples were thoroughly mixed to ensure a standard composition.

The soil vertical profile was obtained by digging 2 m longitudinally. Prior to sampling, the profile was smoothed. Samples were collected from each layer from bottom to top to prevent upper layer soil from affecting lower layers. The



审图号 : GS 京 (2025) 2380 号

Fig. 1 Distribution of soil sampling points in eastern Yunnan Province, China.

Table 1 Statistics of soil types and land use types in the research area

Brown soil		Yellow-brown soil		Yellow soil		Purple soil		Red soil	
Land use type	Sample size	Land use type	Sample size	Land use type	Sample size	Land use type	Sample size	Land use type	Sample size
Forestland	72	Forestland	19	Forestland	30	Forestland	30	Forestland	19
Plantation	14	Plantation	2	Plantation	13	Plantation	6	Plantation	6
Dryland	788	Dryland	151	Dryland	287	Dryland	334	Dryland	236
Grassland	34	Grassland	1	Grassland	18	Grassland	17	Grassland	11
Irrigated land	27	Irrigated land	1	Irrigated land	1	Irrigated land	8	Irrigated land	2

weight of each sample exceeded 1 kg. Each profile was divided into layers at 20 cm intervals, and a thin layer of soil samples was cut from the vertical profile, with 10 samples taken from each profile. All samples were transported to the laboratory and placed in a cool, ventilated location to dry. The samples were ground and sieved through a 200-mesh sieve. During sample collection, key information including sampling point coordinates, crop type, land use type, soil type, and surrounding environmental conditions was documented.

2.3. Measurement of soil properties

SOC was determined using the concentrated sulfuric acid-potassium dichromate wet oxidation method (Walkley and Black 1934), with heat application (170–180°C) in oil for 5 min (Li *et al.* 2018). Soil N was determined using the Kjeldahl method (Bremner 1960). Soil particle size composition was analyzed using the Bouyoucos hydrometer method, classifying soil particles into three categories: clay (<0.002 mm), silt (0.002–0.05 mm), and sand (0.05–2 mm) (Bouyoucos 1962). According to the USDA classification, soils were categorized as sandy, loam, or clay (Eyong and Ofem 2020). Concentrations of P, Al, Ca, Fe, K, Mg, Cr, Cu, Mn, Ni, Pb, Si, Co, Cd, Ti, and V were measured using X-ray fluorescence spectrometry (XRF) (Goldstein *et al.* 1996). The soil-water mixture (1:2.5 ratio) was agitated for 1–2 min, settled for 30 min, and pH was measured using a FE20K pH meter (FE20K FiveEasy Plus, Mettler Toledo, Greifensee, Switzerland) (Li *et al.* 2021). For additional chemical analysis, soil samples were air-dried, ground through a 200-mesh sieve, and dried at 105°C. The concentrations of ferric oxide (Fe_2O_3), potassium oxide (K_2O), calcium oxide (CaO), magnesium oxide (MgO), and Zn in soil samples (3–5 g) were determined through XRF. Mo, Hg, I, and Se concentrations were measured by inductively coupled plasma-mass spectrometry (ICP-MS) (Falciani *et al.* 2000). B concentrations were analyzed using Inductively Coupled Plasma Optical Emission Spectroscopy (Avio 550 Max ICP-OES, PerkinElmer, Shanghai, China) (Yi *et al.* 2023), F was measured by ion chromatography (IC) (Arul Suganthi *et al.* 2023), and S concentrations were determined using a volumetric analytical method (Galindo *et al.* 1969).

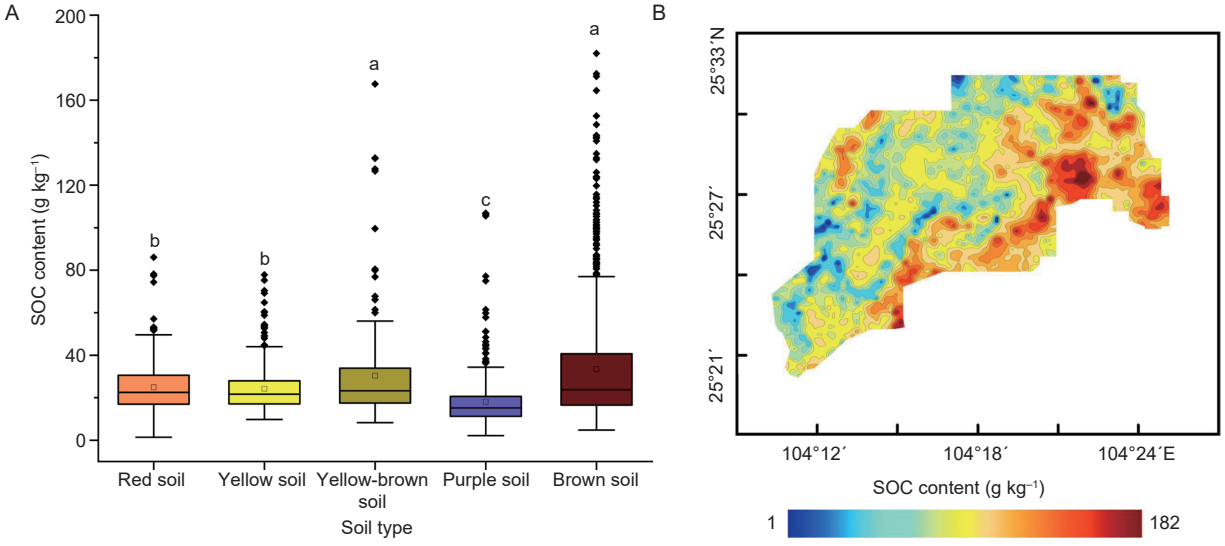
2.4. Data processing and analysis

ArcGIS v.10.5 was employed to map sampling point distribution, and analysis of variance (ANOVA) was performed using SPSS v. 20.0. Duncan's multiple comparison test was utilized to compare groups, with the significance level established at 0.05. The ggpubr package in R (v. 4.3.1) was used to generate a matrix heatmap. Correlation analysis was conducted, and elemental-concentration plots of soil samples were created using Origin 2023.

3. Results

3.1. SOC content of different soil types and SOC spatial distributions

The SOC content exhibited a decreasing trend in the following order: brown soil (33.52±27.57 g kg^{-1})>yellow-brown soil (30.42±23.63 g kg^{-1})>red soil (24.91±12.03 g kg^{-1})>yellow soil (24.20±11.19 g kg^{-1})>purple soil (18.12±12.55 g kg^{-1}) (Fig. 2-A). Brown soil demonstrated 10.2% higher SOC than yellow-brown soil (though not statistically significant; $P>0.05$), and 34.6–85.0% greater SOC compared to other soil types ($P<0.05$). The coefficient of variation reached its maximum in brown soil and minimum in yellow and red soils. SOC concentrations showed no significant difference between brown and yellow-brown soils ($P>0.05$), while both demonstrated significantly higher levels than other soil types ($P<0.05$). Red and yellow soils exhibited comparable SOC levels ($P>0.05$), whereas purple soil displayed significantly lower concentrations ($P<0.05$). SOC content demonstrated notable spatial variability across the study area (104°10′–104°25′E, 25°21′–25°32′N),



审图号：GS 京 (2025) 2380 号

Fig. 2 The distribution of soil organic carbon in the study area. A, soil organic carbon (SOC) content in different soil types in the study area. B, heat map of spatial distribution of SOC. Different lowercase letters denote significant differences ($P<0.05$).

ranging from 1 to 182 g kg^{-1} with a mean of 27.78 g kg^{-1} (Fig. 2-B). High-SOC regions were predominantly located in the northeastern area (104°18′–104°25′E, 25°24′–25°32′N), with maximum SOC content reaching 182 g kg^{-1}. In contrast, low-SOC zones were concentrated in the southwestern region (104°10′–104°15′E, 25°21′–25°24′N), with minimum values of 1 g kg^{-1}. Intermediate SOC levels displayed a heterogeneous spatial distribution, showing gradual transitions from east to west between high- and low-concentration zones, suggesting complex interactions between topographic features and soil properties.

3.2. SOC content of different land use types

Significant variations in SOC content were observed across land use types within each soil category (Fig. 3). In red soils (Fig. 3-A), dryland exhibited significantly higher SOC compared to forestland, plantation and irrigated land (P<0.05), while grassland showed no significant differences from these types. For brown soil (Fig. 3-B), irrigated land demonstrated the highest SOC (P<0.05), followed by dryland, while forestland, grassland, and plantation displayed similar lower values. Yellow soil (Fig. 3-D) exhibited patterns similar to brown soil, i.e., irrigated land showed the highest SOC (P<0.05), dryland ranked second, and forestland/grassland/plantation demonstrated no significant differences. Purple soil (Fig. 3-C) displayed significantly higher SOC in irrigated land compared to forestland, grassland, dryland, and plantation (P<0.05), with no differences among the latter four. In yellow-brown soil (Fig. 3-E), irrigated land similarly showed significantly higher SOC than other land uses (P<0.05), while forestland, grassland, dryland, and plantation maintained similar levels. Notably, brown soil under irrigation exhibited the highest SOC among all sampled sites.

3.3. Correlation between SOC and soil elements

Among the five soil types in the study area, SOC demonstrated significant pairwise positive correlations with N, S, and Se (P<0.01, r_N=0.87, r_S=0.65, r_{Se}=0.78; Fig. 4), and all four elements showed negative correlations with Mg (P<0.01, r_c=−0.44, r_N=−0.54, r_S=−0.52, r_{Se}=−0.68; Fig. 4).

3.4. Correlation of SOC with soil texture, altitude and pH

Soil texture exhibited variation among different soil types. Purple soil predominantly consisted of sand (79.0%). In yellow soil, sand and silt comprised 47.6 and 31.4%, respectively. Red soil primarily contained silt and sand, constituting 43.6 and 37.7%, respectively. The particle distribution in brown and yellow-brown soils demonstrated

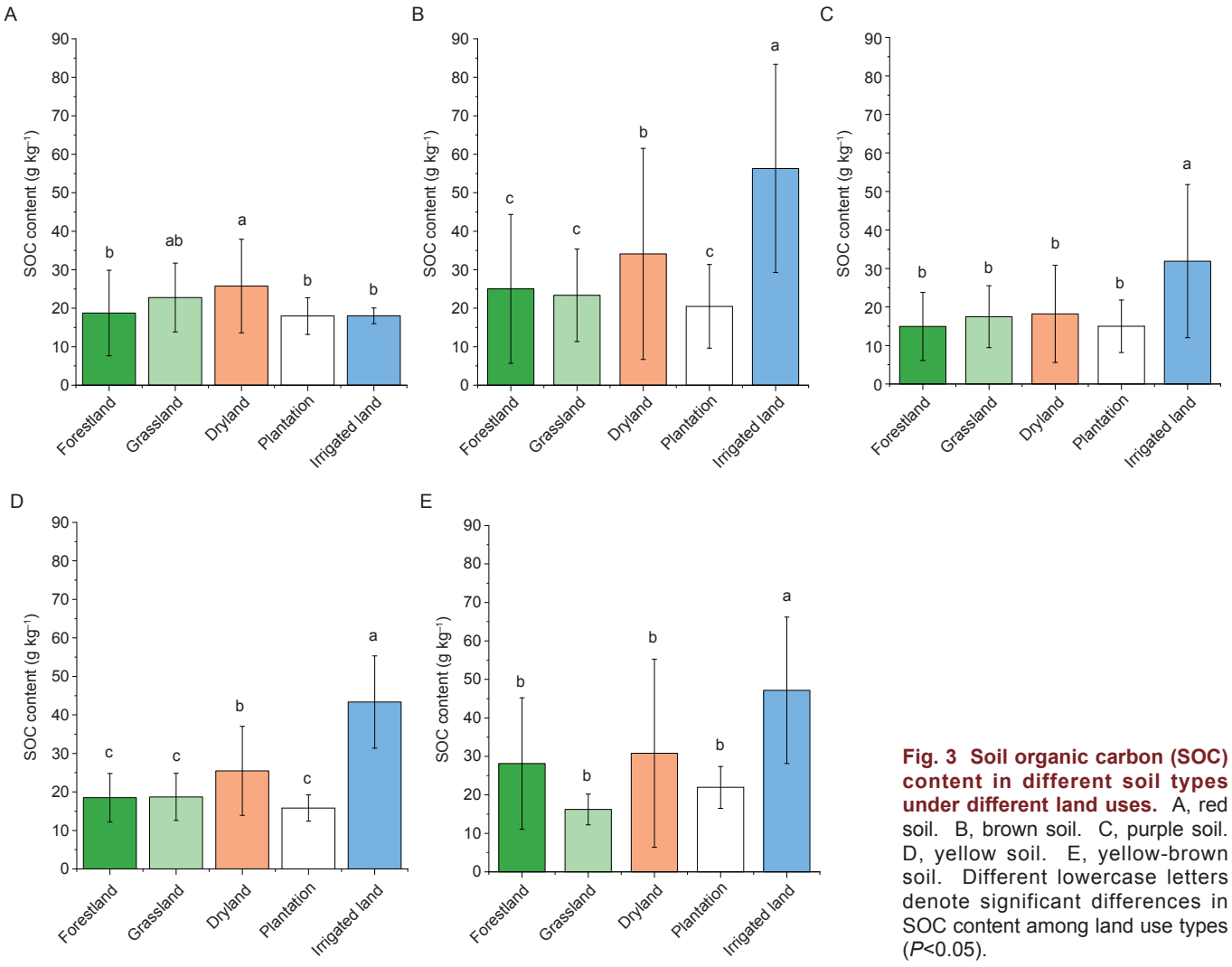


Fig. 3 Soil organic carbon (SOC) content in different soil types under different land uses. A, red soil. B, brown soil. C, purple soil. D, yellow soil. E, yellow-brown soil. Different lowercase letters denote significant differences in SOC content among land use types (P<0.05).

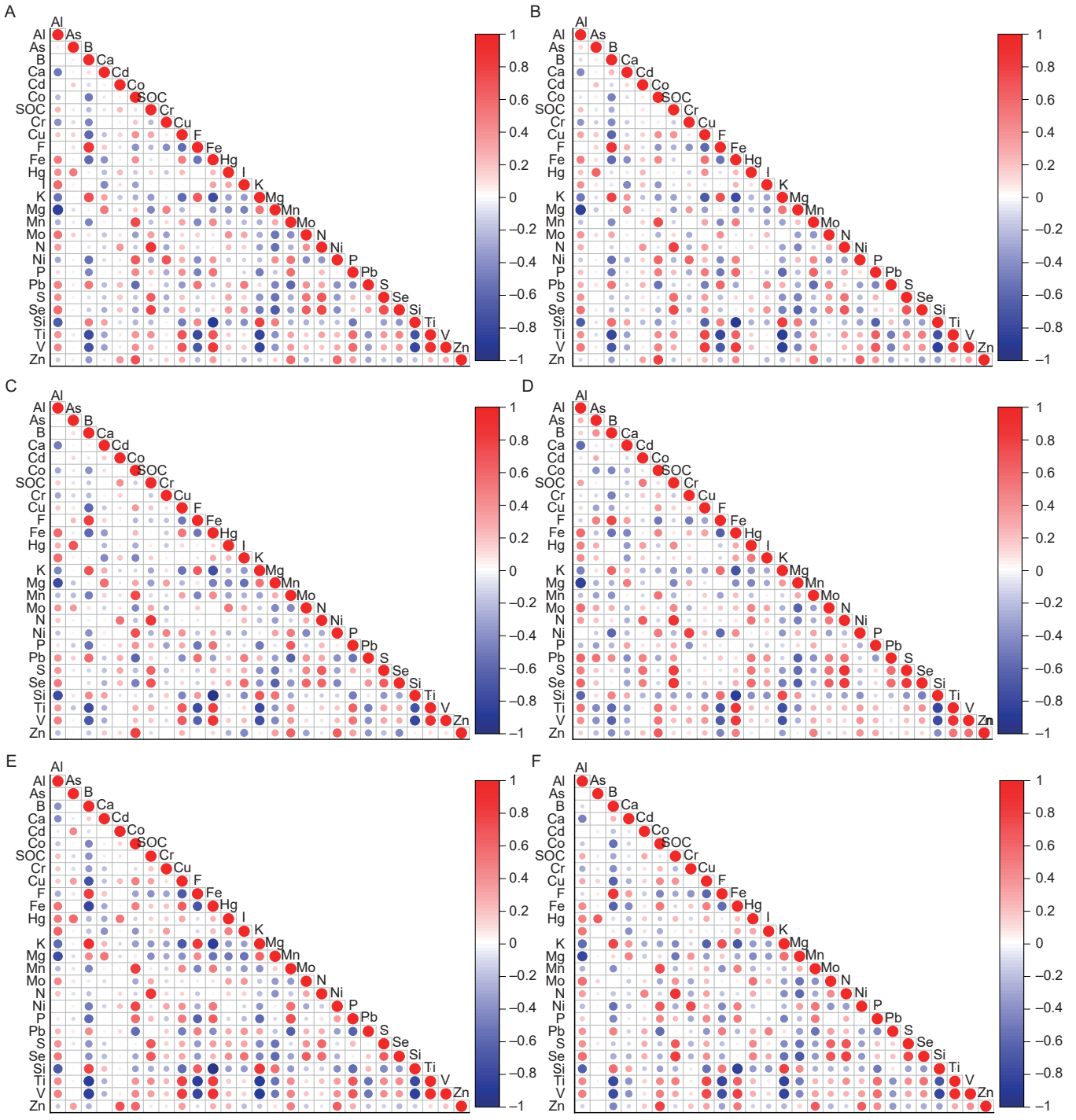


Fig. 4 Correlations between soil organic carbon (SOC) and various elements in different soil types in the study area. A, full soil type. B, yellow-brown soil. C, red soil. D, purple soil. E, yellow soil. F, brown soil.

similarity (Fig. 5-A). Soil texture influences surface SOC content (Fig. 5-B). Loam exhibits the highest SOC content ((31.35±25.74) g kg^{-1}), demonstrating substantial SOC enrichment capacity. The SOC content in sandy ((26.61±21.15) g kg^{-1}) and clay ((24.13±13.85) g kg^{-1}) textures was notably lower than in loam (P<0.05), though without significant difference between them. The interaction of soil type and texture influences the spatial distribution of SOC (Fig. 5-C), displaying binary collaborative regulation characteristics. The brown soil-loam combination demonstrates higher SOC content compared to other soil type-texture combinations, creating SOC enrichment hotspots. The clay combination of yellow soil and various texture combinations of purple soil generally exhibit lower SOC content. The interaction between land use types and soil texture determines SOC accumulation patterns (Fig. 5-D). Irrigated land maintained the highest SOC content across all texture conditions, showing significantly higher levels in sandy and clayey soils compared to other land use types (P<0.05). The clay soil-irrigated land combination produced a

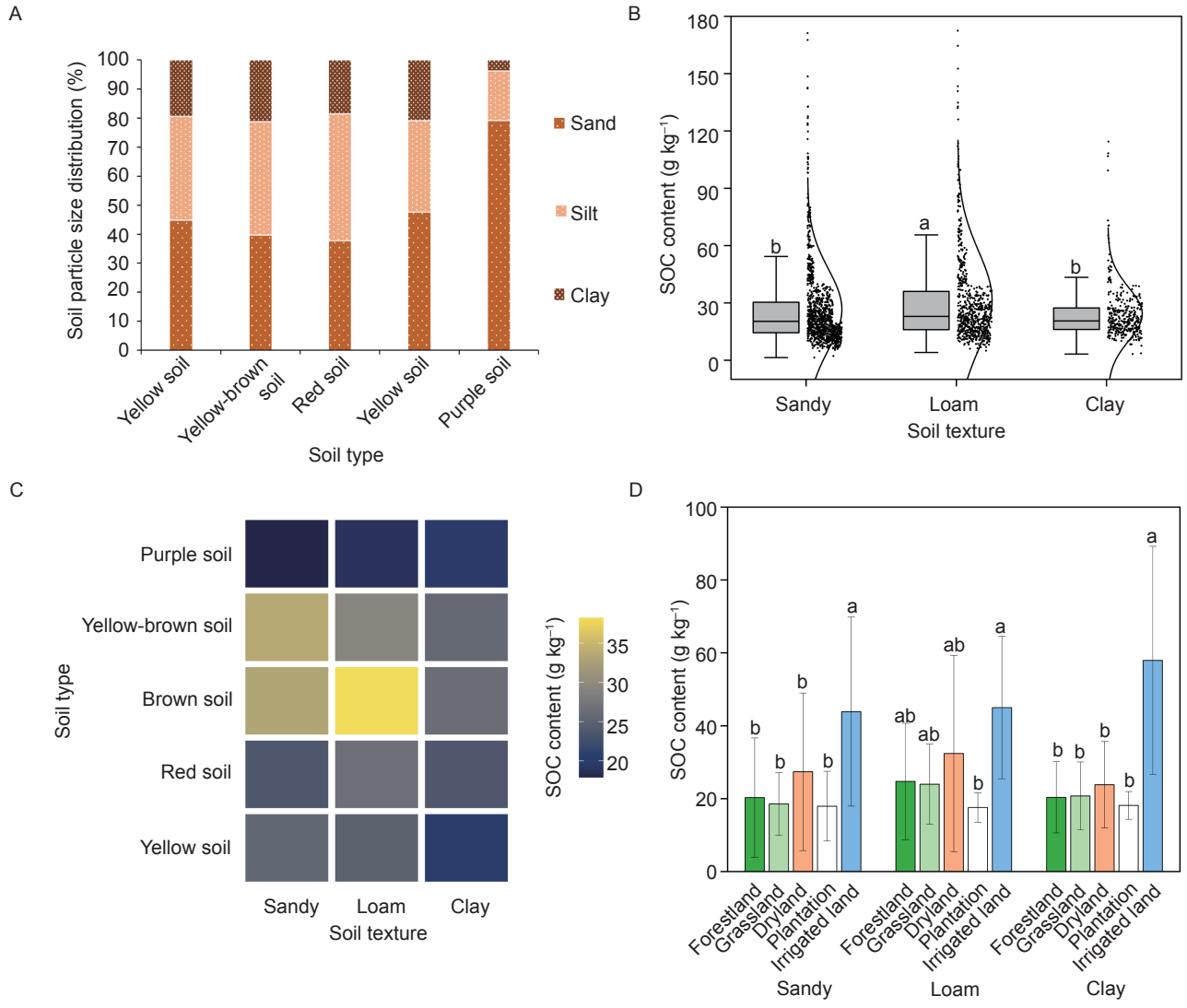


Fig. 5 Soil organic carbon (SOC) distribution across soil texture classes. A, soil particle size distribution of main soil types in the study area. B, SOC distribution across soil textural classes. C, the interactive effects of soil type and textural composition on SOC patterns. D, stratified distribution of SOC by land use type and textural classes. Different lowercase letters in Fig. 5-B indicate significant differences among soil texture, while in Fig. 5-D, different lowercase letters indicate significant differences in different land use types under the same soil texture (P<0.05).

notable SOC enrichment hotspot ((57.93±31.30) g kg^{-1}). The soils in the study area were acidic (pH 4.02–7.50). The SOC content of different soil types showed no correlation with pH (Fig. 6). Linear regression analysis revealed that while all five soil types demonstrated a significant decrease in SOC with increasing altitude (P<0.001), the altitude factors exhibited relatively weak explanatory power for SOC variability (R^2=0.046–0.093) (Fig. 7).

4. Discussion

4.1. Analysis of differences in surface SOC content under each soil type

Multiple factors including soil-forming parent material, soil properties, and fertilizer application affect SOC content across different soil types (Ni *et al.* 2022; Ortner *et al.* 2022; Amaleviciute-Volunge *et al.* 2024). Soil Cd concentrations influence bacterial community structures, which subsequently affects SOC immobilization and decomposition in various soil types (Meng *et al.* 2023). Agricultural land in the study area received N fertilizer and farmyard manure applications, which generally increased SOC content across all soil types (Chan *et al.* 2010; Jiang *et al.* 2022; Just *et al.* 2024). The impact of N input on SOC content varies by soil type (Ni *et al.* 2022), representing a primary factor in SOC content variation among soil types in this study.

In this study, the SOC content in purple soil was lower compared to other soil types (Fig. 2-A), a finding consistent with previous research (Chen F 2022; Li *et al.* 2023). Purple soil develops in subtropical regions where exposed purple parent rock undergoes weathering through temperature, light, and water processes. Its limited soil formation time and developmental processes result in low fertility (Wang *et al.* 2018). Purple soil zones experience significant soil erosion and fertility loss due to steep topography, high precipitation,

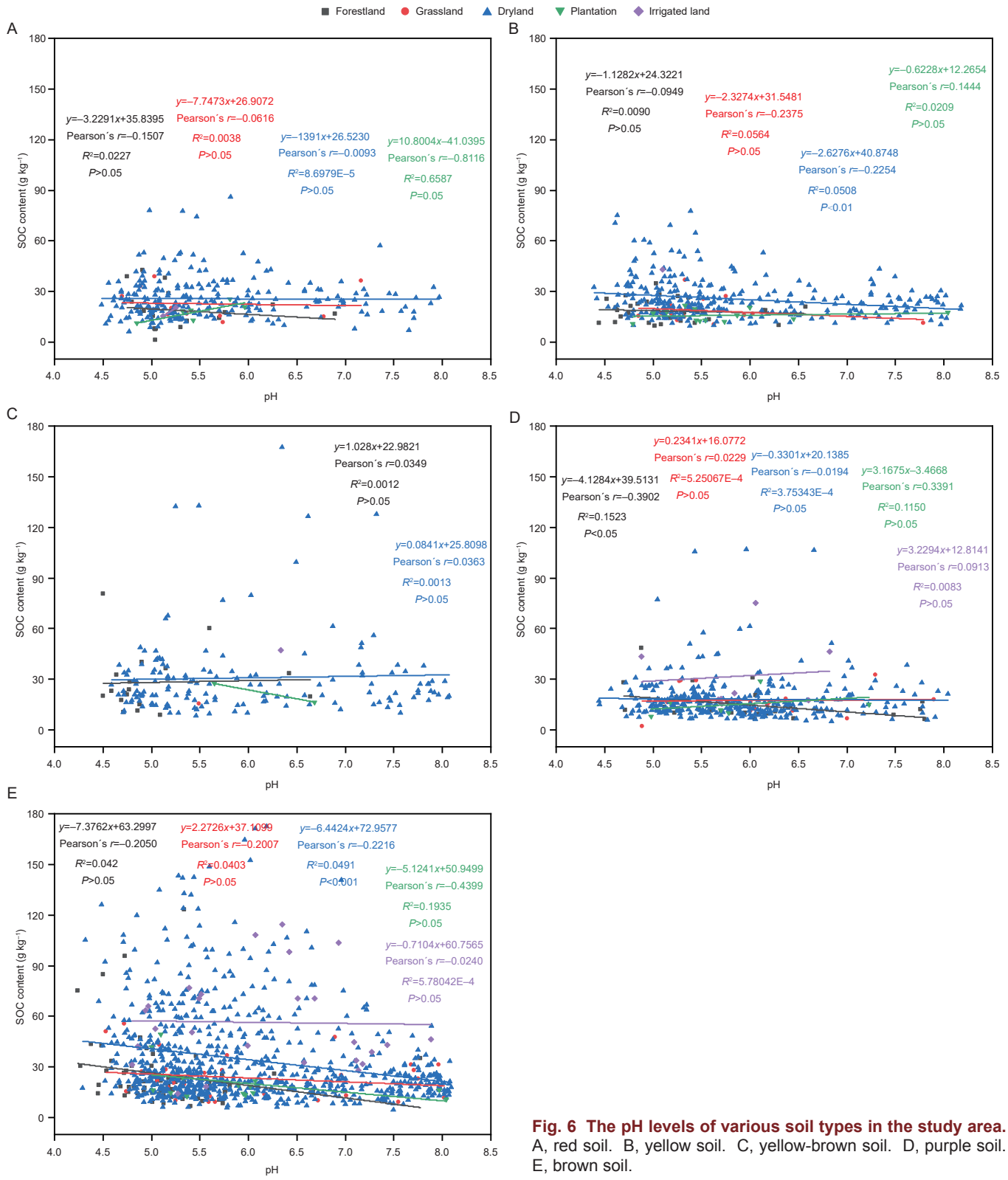


Fig. 6 The pH levels of various soil types in the study area. A, red soil. B, yellow soil. C, yellow-brown soil. D, purple soil. E, brown soil.

and suboptimal land use practices (Liang *et al.* 2022). The soil is characteristically shallow and loose, with poor water permeability in the shale layer. In purple soil regions, rainfall occurs frequently and concentrates in summer, while silt mesocosm development is more pronounced (Shen *et al.* 2021). Consequently, purple soil demonstrates weak erosion resistance and easily degradable aggregate structure, resulting in relatively low SOC content in the topsoil layer. Sandy soils exhibit significantly higher organic carbon mineralization rates compared to clay soils (Liddle *et al.* 2020; Medeiros *et al.* 2022), with values up to twice as high in sandy substrates (Frøseth *et al.* 2022). Red and yellow soils share ferro-aluminous properties (Schaetzl and Anderson 2005) but differ in soil texture (Fig. 5-A). Yellow soil contains more sand

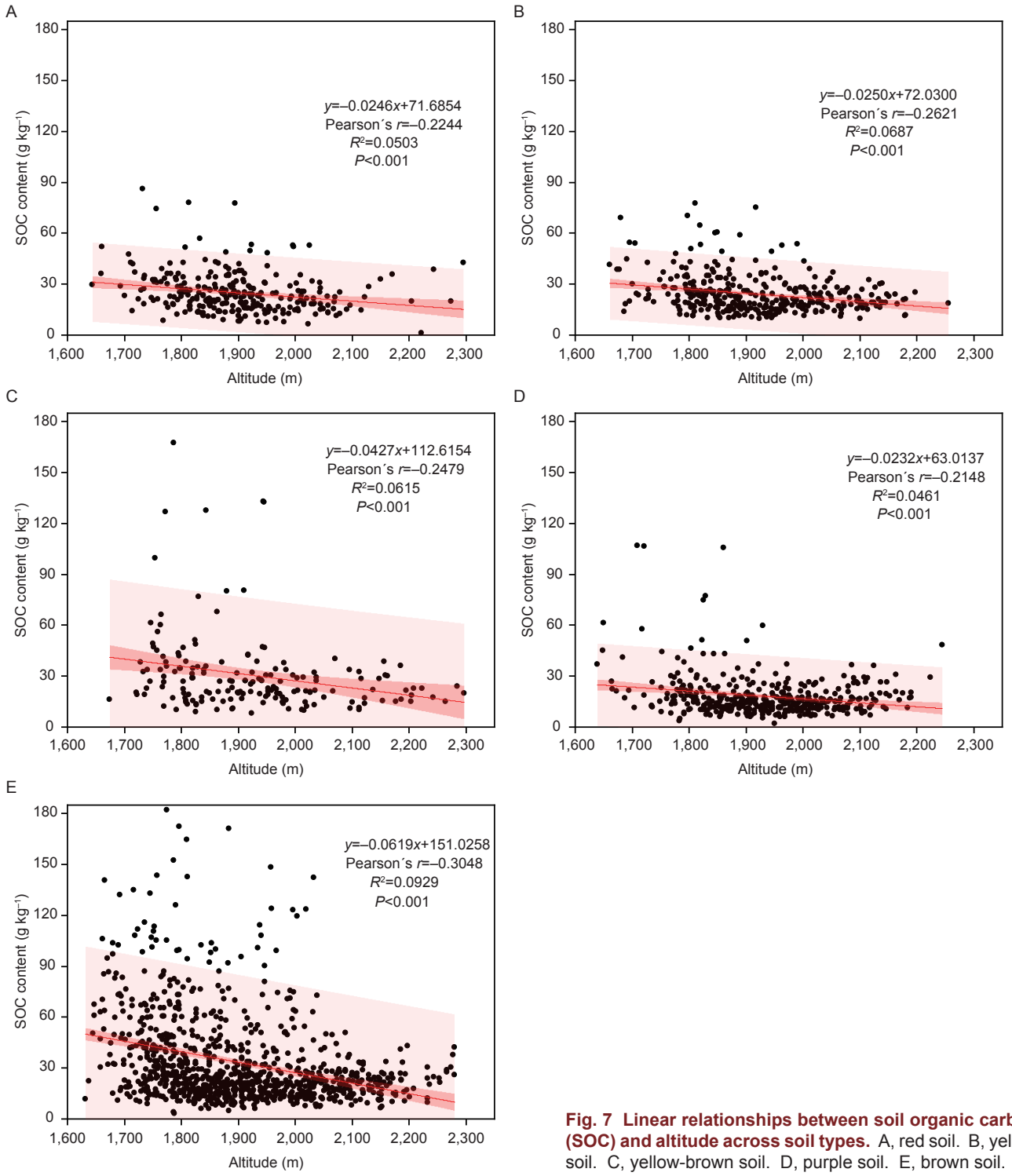


Fig. 7 Linear relationships between soil organic carbon (SOC) and altitude across soil types. A, red soil. B, yellow soil. C, yellow-brown soil. D, purple soil. E, brown soil.

than red soil (Fig. 5-A). While red soil has less sand content, it shows lower clay proportion, whereas brown soil exhibits higher clay and silt content, corresponding to elevated SOC levels. Furthermore, brown soil and yellow-brown soil in this study are primarily leached soils. The substantial SOC accumulation in leached soils results from secondary clay mineral enrichment through leaching processes and iron-aluminum-organic matter complex protection mechanisms, significantly increasing mineral-bound organic carbon proportion (MAOC>50%) (Li *et al.* 2023).

4.2. Analysis of differences in SOC content by land use type under each soil type

The observed effects of different land use types on SOC in this study resulted from anthropogenic disturbances (Anderson and Coleman 1985). Across the five soil types, irrigated land demonstrated substantially higher SOC content compared to other land use types (Fig. 3), attributable to the positive correlation between SOC fraction and soil water content (Yang *et al.* 2020). Adequate water availability creates favorable conditions for ecological

processes including microbial decomposition, enabling microorganisms to maintain high activity levels and promote SOC accumulation (Fernández *et al.* 2021). Unlike drylands with limited water resources, irrigated land maintains soil water content at levels more conducive to soil carbon fixation (Ye *et al.* 2023). Increasing dryland SOC content may be achieved through soil water addition (Ortiz *et al.* 2022). The study area features predominantly contiguous terrace distributions in drylands. During rainy seasons, surface SOC in terraces migrates to lower soil profile levels. Topsoil and organic matter transport from upper slopes results in higher SOC content in low-lying terraced drylands compared to elevated locations, explaining the substantial SOC content variation in agricultural fields, as noted by Chadwick *et al.* (2016). Cropland exhibited higher SOC content than woodlands and grasslands due to applications of farmyard manure, N fertilizer, and chemical fertilizer. Fertilizer application enhances SOC content (Jordon *et al.* 2024; Shi *et al.* 2024; Li and Li 2025). Sustained fertilization increases soil carbon sequestration rates and capacity, while chemical fertilizer application also elevates SOC content (Smith *et al.* 2020; Shah *et al.* 2021; Liu *et al.* 2022; Zhou *et al.* 2022; Xu *et al.* 2025). Human irrigation and fertilization practices have markedly improved agricultural land water and nutrient conditions compared to grasslands. While plantations receive fertilization, they experience greater human interference, including fruit tree pruning for growth control and other operations that reduce soil organic matter input. Mechanical soil disturbances (e.g., tillage) typically cause significant decreases in SOC stocks, with reductions exceeding 20% in intensively managed agroecosystems (Krauss *et al.* 2022; Kutova *et al.* 2024). Therefore, reducing deep plowing in plantations and implementing debris and tree branch backfilling can enhance plantation soil SOC content.

4.3. Analysis of other factors affecting soil organic carbon

This study revealed a significant positive correlation between SOC content and soil N, S, and Se (Fig. 4). Selenium demonstrates a significant impact on plant growth at appropriate concentrations, primarily by enhancing plant resistance and increasing chlorophyll content (Han *et al.* 2013). As N serves as the essential element for chlorophyll synthesis in plants (He *et al.* 2022), the synergistic interactions between Se and N substantially promote SOC accumulation, particularly in dryland soils with high Se/N availability. These elements are prevalent in the study area. The application of N fertilizer and farmyard manure in drylands provides substantial N supplementation (Laub *et al.* 2023). In conjunction with S, these soil elements are vital for plant growth and metabolism, facilitating SOC synthesis in drylands (Zenda *et al.* 2021). Research has demonstrated that N enrichment significantly increases SOC content (Bai *et al.* 2021; Tang *et al.* 2023). Plant-active selenium serves as a permissible selenium source for humans and animals, while nitrogen fertilization in the study area's drylands enhances plant selenium uptake and content (Kong *et al.* 2023). Studies have identified strong correlations between soil C, N, and selenium, with organic carbon showing significant positive correlation with soil selenium content, aligning with the present findings (Zhou *et al.* 2014; Li *et al.* 2017). Nitrogen fertilizer application thus facilitates high selenium maize production and agricultural product improvement while increasing soil organic carbon. Variations in soil-forming materials, climate, topography, vegetation cover, and human intervention create spatial heterogeneity in SOC at multiple scales (Wang *et al.* 2023), resulting in a spatial distribution pattern of SOC in the study area with higher values in the northeast and lower values in the southwest (Fig. 2-B).

The SOC content in loam significantly exceeds that of sandy soil and clay soil (Fig. 5-B), primarily due to its balanced particle composition's synergistic effect. This combination creates a distinctive microenvironment: the moderate pore structure ensures sufficient aeration for plant growth (increasing carbon input) (Virto *et al.* 2008) while reducing organic matter leaching through powder and clay particle surface adsorption (Cotrufo *et al.* 2019). Furthermore, it facilitates water-stable aggregate formation, providing effective physical protection for organic carbon (Lehmann *et al.* 2020). This "input-preserve" equilibrium renders SOC accumulation efficiency in loam notably higher than in sandy soil (where excessive aeration accelerates organic matter decomposition) (Angst *et al.* 2021) and clay (where insufficient aeration restricts root activity and carbon input) (Six *et al.* 2000). Consequently, loam texture in brown soil of the leached soil class exhibits higher SOC content than various textures in other soil types including red soil, yellow soil, yellow-brown soil and purple soil (Fig. 5-C). The SOC content of sandy and clay irrigated land significantly exceeded that of the other four land use types (Fig. 5-D, $P<0.05$), further validating irrigation's positive effect on SOC and providing evidence for green and low-carbon agriculture. Analysis of 2,132 sample points reveals an altitude range of 1,632–2,297 m, with a significant weak negative correlation between altitude and SOC (Fig. 7, $P<0.001$), indicating decreasing SOC content with increasing elevation, manifesting as slope foot>slope middle>slope top (Luo *et al.* 2024). During 2011–2020, the study area's average annual temperature varied between 17.0°C–17.9°C, with annual precipitation ranging from 644–1,167 mm. The relatively narrow research area leads to no significant differences.

5. Conclusion

The study area exhibited a mean SOC content of 27.78 g kg^{-1}, with surface soil content decreasing in the order of brown soil>yellow-brown soil>red soil>yellow soil>purple soil. Among the five soil types, irrigated land showed the highest SOC content, while drylands demonstrated the highest SOC content among agricultural land uses. Increased soil water content in dryland regions would enhance soil SOC content in agricultural lands. Nitrogen fertilizer application facilitates high selenium maize production and agricultural product improvement while increasing SOC content.

Acknowledgements

This research was funded by the Yunnan Provincial Key Programs for Basic Research Project, China

(202301AS070087), the Yunnan Provincial R & D Program, China (202405AF140014 and 202302AO370015), and the National Natural Science Foundation of China (42307058).

Declaration of competing interest

The authors declare that they have no conflict of interest.

Declaration of generative AI and AI-assisted technologies in scientific writing

During the preparation of this manuscript, the authors used DeepSeek to assist in improving the clarity and readability of the language. All content generated was carefully reviewed and revised by the authors as necessary, and the authors take full responsibility for the final content of the article.

References

Amaleviciute-Volunge K, Tripolskaja L, Kazlauskaite-Jadzevice A, Slepetiene A, Baksiene E. 2024. Effect of long-term different land uses on improving stable humic compounds in Arenosol. *Agriculture*, **14**, 250.

Anderson D W, Coleman D C. 1985. The dynamics of organic matter in grassland soils. *Journal of Soil and Water Conservation*, **40**, 211–216.

Angst G, Pokorný J, Mueller C W, Prater I, Preusser S, Kandeler E, Meador T, Straková P, Hájek T, Buiten G V, Angst Š. 2021. Soil texture affects the coupling of litter decomposition and soil organic matter formation. *Soil Biology and Biochemistry*, **159**, 108302.

Arul Suganthi C, Raut V V, Bharti N K, Thakur U K, Sri Renganathan P, Jeyakumar S, Saxena M K. 2023. Separation of fluoride in the presence of large amounts of organic acids by ion chromatography. *Separation Science and Technology*, **58**, 2759–2766.

Bai T S, Wang P, Ye C L, Hu S J. 2021. Form of nitrogen input dominates N effects on root growth and soil aggregation: A meta-analysis. *Soil Biology and Biochemistry*, **157**, 108251.

Bouyoucos G J. 1962. Hydrometer method improved for making particle size analysis of soils. *Agronomy Journal*, **54**, 464–465.

Bremner J M. 1960. Determination of nitrogen in soil by the Kjeldahl method. *The Journal of Agricultural Science*, **55**, 11–33.

Chadwick K, Asner D, Gregory P. 2016. Tropical soil nutrient distributions determined by biotic and hillslope processes. *Biogeochemistry*, **127**, 273–289.

Chen F. 2022. Spatial distribution characteristics and influencing factors of soil organic carbon in karst region. Ph D thesis, Guizhou University, China. (in Chinese)

Chan K Y, Oates A, Li G D, Conyers M K, Prangnell R J, Poile G, Liu D L, Barchia I M. 2010. Soil carbon stocks under different pastures and pasture management in the higher rainfall areas of south-eastern Australia. *Soil Research*, **48**, 7–15.

Cotrufo M F, Ranalli M G, Haddix M L, Six J, Lugato E. 2019. Soil carbon storage informed by particulate and mineral-associated organic matter. *Nature Geoscience*, **12**, 989–994.

Don A, Schumacher J, Freibauer A. 2011. Impact of tropical land-use change on soil organic carbon stocks — A meta-analysis. *Global Change Biology*, **17**, 1658–1670.

Ebabu K, Tsunekawa A, Haregeweyn N, Adgo E, Meshesha D T, Aklog D, Masunaga T, Tsubo M, Sultan D, Fenta A A, Yibeltal M. 2020. Exploring the variability of soil properties as influenced by land use and management practices: A case study in the Upper Blue Nile basin, Ethiopia. *Soil and Tillage Research*, **200**, 104614.

Eyong M O, Ofem K I. 2020. Soil mechanical composition and texture as indices for on-site and field precise choice of land use type to adopt. *Asian Soil Resources Journal*, **4**, 28–43.

Falciani R, Novaro E, Marchesini M, Gucciardi M. 2000. Multi-element analysis of soil and sediment by ICP-MS after a microwave assisted digestion method. *Journal of Analytical Atomic Spectrometry*, **15**, 561–565.

Fernández R, Belmonte V, Quiroga A, Lobartini C, Noellemeyer E. 2021. Land-use change affects soil hydro-physical properties in Mollisols of semiarid Central Argentina. *Geoderma Regional*, **25**, e00394.

Fick S E, Hijmans R. 2017. WorldClim 2: New 1-km spatial resolution climate surfaces for global land areas. *International Journal of Climatology*, **37**, 4302–4315.

Frøseth R B, Thorup-Kristensen K, Hansen S, Bleken M A. 2022. High N relative to C mineralization of clover leaves at low temperatures in two contrasting soils. *Geoderma*, **406**, 115483.

Galindo G G, Appelt H, Schalscha E B. 1969. Sulfur determination in soil extracts by an indirect atomic absorption spectrophotometric method. *Soil Science Society of America Journal*, **33**, 974–975.

Gao Y, Zhang Y, Liu J, An Y, Ma H, Tong S. 2025. Investigating the compensatory effect of legume reseeding on soil organic carbon loss under tillage management in a saline-alkali grassland in the semi-arid region. *Ecological Engineering*, **210**, 107441.

Goldstein S J, Slemmons A K, Canavan H E. 1996. Energy-dispersive X-ray fluorescence methods for environmental characterization of soils. *Environmental Science & Technology*, **30**, 2318–2321.

Guillaume T, Kotowska M M, Hertel D, Knohl A, Krashevska V, Murtilaksono K, Scheu S, Kuzyakov, Y. 2018. Carbon costs and benefits of Indonesian rainforest conversion to plantations. *Nature Communications*, **9**, 2388.

Harris I, Osborn T J, Jones P, Lister D. 2020. Version 4 of the CRU TS monthly high-resolution gridded multivariate climate dataset. *Scientific Data*, **7**, 109.

Han D, Li X, Xiong S, Tu S, Chen Z, Li J, Xie Z. 2013. Selenium uptake, speciation and stressed response of *Nicotiana tabacum* L. *Environmental and Experimental Botany*, **95**, 6–14.

He S, Zhao Y Y, Liu C P, Li Z H, Zhang Z Y, Li B, Tang X D. 2022. An exploration into the relationship between mineral elements (nitrogen and phosphorus) and nutritional quality in soil–watermelon (*Citrullus lanatus*) system. *Journal of Analytical Science and Technology*, **13**, 48.

Just B S, Marks E A N, Roquer-Beni L, Llenas L, Ponsà S, Vilaplana R. 2024. Biofertilization increases soil organic carbon concentrations: Results of a meta-analysis. *International Journal of Agricultural Sustainability*, **22**, 2361578.

Jiang Y, Zhang S, Gao B, Wei R, Ding X. 2022. Fe (II)-OM complexes formed by straw returning combined with optimized nitrogen fertilizer could be beneficial to nitrogen storage in saline-alkaline paddy soils. *Agronomy*, **12**, 2295.

Jordon M W, Buffet J C, Dungait J A, Galdos M V, Garnett T, Lee M R F, Lynch J, Röös E, Searchinger T D, Smith P, Godfray H C J. 2024. A restatement of the natural science evidence base concerning grassland management, grazing livestock and soil carbon storage. *Proceedings of the Royal Society* (B: Biological Sciences), **291**, 20232669.

Kong W L, Huo R W, Lu Y, Fan Z J, Yue R Q, Ren A X, Li L H, Ding P C, Ren Y K, Gao Z Q, Sun M. 2023. Nitrogen application can optimize form of selenium in soil in selenium-rich areas to affect selenium absorption and accumulation in black wheat. *Plants*, **12**, 4160.

Krauss M, Wiesmeier M, Don A, Cuperus F, Gattinger A, Gruber S, Haagsma W K, Peigné J, Chiodelli Palazzoli M, Schulz F, van der Heijden M G A, Vincent-Caboud L, Wittwer R A, Zikeli S, Steffens M. 2022. Reduced tillage in organic farming affects soil organic carbon stocks in temperate Europe. *Soil and Tillage Research*, **216**, 105262.

Kutova A, Shediei L, Skrylnik I, Mykhaylyn V, Semenenko I. 2024. Soil carbon sequestration and stocks following land-use types change. *Scientific Papers* (Series A. Agronomy), **67**, 129–135.

Lal R. 2004. Soil carbon sequestration to mitigate climate change. *Geoderma*, **123**, 1–22.

Laub M, Corbeels M, Ndungu S M, Mucheru-Muna M W, Mugendi D, Necpalova M, Broek M V D, Waswa W, Vanlauwe B, Six J. 2023. Combining manure with mineral N fertilizer maintains maize yields: Evidence from four long-term experiments in Kenya. *Field Crops Research*, **291**, 108788.

Lehmann J, Hansel C M, Kaiser C, Kleber M, Maher K, Manzoni S, Nunan N, Reichstein M, Schimel J P, Torn M S, Wieder W R, Kögel-Knabner I. 2020. Persistence of soil organic carbon caused by functional complexity. *Nature Geoscience*, **13**, 529–534.

Li A W, Ran M, Song L Y, Xue J L, Zang Y Y, Li C J, Deng Q, Fang H Y, Dai T F, Li Q Q. 2023. Spatial distribution characteristics and influencing factors of cropland topsoil organic carbon content in the Sichuan Basin. *Resources and Environment in the Yangtze Basin*, **32**, 1102–1112. (in Chinese)

Li H Q, Shen Y J, Wang W L, Wang H T, Li H, Su J Q. 2021. Soil pH has a stronger effect than arsenic content on shaping plastisphere bacterial communities in soil. *Environmental Pollution*, **287**, 117339.
Li J, Wen Y C, Li X H, Li Y T, Yang X D, Lin Z A, Song Z Z, Cooper J M, Zhao B Q. 2018. Soil labile organic carbon fractions and soil organic carbon stocks as affected by long-term organic and mineral fertilization regimes in the North China Plain. *Soil and Tillage Research*, **175**, 281–290.
Li L, Qin F C, Jiang L, Yao X L, Wang X. 2019. Effects of land use type and terrain on soil organic carbon (SOC) content in semi-arid region. *Soil*, **51**, 406–412. (in Chinese)
Li Y, Li Y. 2025. Nitrogen addition enhances soil carbon and nutrient dynamics in Chinese croplands: A machine learning and nationwide synthesis. *Carbon Balance and Management*, **20**, 15.
Li Z, Liang D L, Peng Q, Cui Z W, Huang J, Lin Z Q. 2017. Interaction between selenium and soil organic matter and its impact on soil selenium bioavailability: A review. *Geoderma*, **295**, 69–79.
Li Z W, Wang S G, Chen X L, Nie X D, Zhang Y, Liu G P, Zeng W Y. 2014. Effect of Land use type of red soil hilly region on distribution of soil labile organic carbon properties under the condition of soil erosion. *Journal of Hunan University* (Natural Sciences), **41**, 88–93. (in Chinese)
Liddle K, McGonigle T, Koiter A. 2020. Microbe biomass in relation to organic carbon and clay in soil. *Soil Systems*, **4**, 41.
Liu Q, Yu Z Y, Wang X M, Zhao S L. 2022. Organic fertilizer increases soil organic carbon and crop yield in four-year tillage and crop rotations on the Loess Plateau, China. *Applied Ecology & Environmental Research*, **20**, 4271–4282.
Liang K, He X, He B, Guo X, Li T. 2022. Runoff-associated nitrogen and phosphorus losses under natural rainfall events in purple soil area: The role of land disturbance and slope length. *Water Supply*, **22**, 1995–2007.
Luo B L, Li J W, Tang J H, Wei C F, Zhong S Q. 2024. Microtopography effects on pedogenesis in the mudstone-derived soils of the hilly mountainous regions. *Scientific Reports*, **14**, 11998.
Luo X Z, Zhang L L, Lin Y B, Wen D Z, Hou E Q. 2023. Nitrogen availability mediates soil organic carbon cycling in response to phosphorus supply: A global meta-analysis. *Soil Biology and Biochemistry*, **185**, 109158.
Medeiros A D S, Soares A A S, Maia S M F. 2022. Soil carbon stocks and compartments of organic matter under conventional systems in Brazilian semi-arid region. *Revista Caatinga*, **35**, 697–710.
Meng Q Y, Diao T T, Yan L, Sun Y B. 2023. Effects of single and combined contamination of microplastics and cadmium on soil organic carbon and microbial community structural: A comparison with different types of soil. *Applied Soil Ecology*, **183**, 104763.
Ni H, Liu C, Sun B, Liang Y. 2022. Response of global farmland soil organic carbon to nitrogen application over time depends on soil type. *Geoderma*, **406**, 115542.
Nyaupane K, Mishra U, Tao F, Yeo K, Riley W J, Hoffman F M, Gautam S. 2024. Observational benchmarks inform representation of soil organic carbon dynamics in land surface models. *Biogeosciences*, **21**, 5173–5183.
Nuralykyzy B, Nurzhan A, Li N, Huang Q, Zhu Z L, An S S. 2023. Influence of land use types on soil carbon fractions in the Qaidam Basin of the Qinghai-Tibet Plateau. *Catena*, **231**, 107273.
Ortiz A C, Jin L X, Ogrinc N, Kaye J, Krajnc B, Ma L. 2022. Dryland irrigation increases accumulation rates of pedogenic carbonate and releases soil abiotic CO_2. *Scientific Reports*, **12**, 464.
Ortner M, Seidel M, Semella S, Udelhoven T, Vohland M, Thiele-Bruhn S. 2022. Content of soil organic carbon and labile fractions depend on local combinations of mineral-phase characteristics. *Soil*, **8**, 113–131.
Poeplau C, Don A. 2015. Carbon sequestration in agricultural soils via cultivation of cover crops — A meta-analysis. *Agriculture, Ecosystems & Environment*, **200**, 33–41.
Raza S, Miao N, Wang P Z, Ju X T, Chen Z J, Zhou J B, Kuzyakov Y. 2020. Dramatic loss of inorganic carbon by nitrogen-induced soil acidification in Chinese croplands. *Global Change Biology*, **26**, 3738–3751.
Roe S, Streck C, Beach R, Busch J, Chapman M, Daioglou V, Deppermann A, Doelman J, Emmet-Booth J, Engelmann J, Fricko O, Frischmann C, Funk J, Grassi G, Griscom B, Havlik P, Hanssen S, Humpenöder F, Landholm D, Lomax G, *et al.* 2021. Land-based measures to mitigate climate change: Potential and feasibility by country. *Global Change Biology*, **27**, 6025–6058.
Schaetzl R, Anderson S. 2005. *Soils*: *Genesis and Geomorphology*. Cambridge University Press, Cambridge.
Shah S A A, Xu M, Abrar M M, Mustafa A, Fahad S, Shah T, Shah S A A, Yan X Y, Zhou W, Zhang S L, Nan S, Shi W Q. 2021. Long-term fertilization affects functional soil organic carbon protection mechanisms in a profile of Chinese Loess Plateau soil. *Chemosphere*, **267**, 128897.
Shen J, Wang X G, Ma H, 2021. Effects of fertilizer application on the process of soil organic carbon loss in a purple soil farmland. *Chinese Journal of Ecological Agriculture*, **29**, 1571–1581. (in Chinese)
Shi T S, Collins S L, Yu K, Peñuelas J, Sardans J, Li H, Ye J S. 2024. A global meta-analysis on the effects of organic and inorganic fertilization on grasslands and croplands. *Nature Communications*, **15**, 3411.
Si Q T N, Chen K L, Wei B, Zhang Y W, Sun X, Liang J Y. 2024. Dissolved carbon flow to particulate organic carbon enhances soil carbon sequestration. *Soil*, **10**, 441–450.
Six J, Paustian K, Elliott E T, Combrink C. 2000. Soil structure and organic matter I. Distribution of aggregate-size classes and aggregate-associated carbon. *Soil Science Society of America Journal*, **64**, 681–689.
Smith P, Soussana J F, Angers D, Schipper L, Chenu C, Rasse D P, Batjes N H, Egmond F V, McNeill S, Kuhnert M, Arias-Navarro C, Olesen J E, Chirinda N, Fornara D, Wollenberg E, Álvaro-Fuentes J, Sanz-Cobena A, Klumpp K. 2020. How to measure, report and verify soil carbon change to realize the potential of soil carbon sequestration for atmospheric greenhouse gas removal. *Global Change Biology*, **26**, 219–241.
Tang B, Rocci K S, Lehmann A, Rillig M C. 2023. Nitrogen increases soil organic carbon accrual and alters its functionality. *Global Change Biology*, **29**, 1971–1983.
Udom B E, Ogunwole J O. 2015. Soil organic carbon, nitrogen, and phosphorus distribution in stable aggregates of an Ultisol under contrasting land use and management history. *Journal of Plant Nutrition and Soil Science*, **178**, 460–467.
Virto I, Barré P, Chenu C. 2008. Microaggregation and organic matter storage at the silt-size scale. *Geoderma*, **146**, 326–335.
Walkley A J, Black I A. 1934. An examination of the degtjareff method for determining soil organic matter, and a proposed modification of the chromic acid titration method. *Soil Science*, **37**, 29–38.
Wang H L, Wang J C, Zhang Y, He G X, Wen S Z. 2023. Spatial distribution of soil organic carbon and its response to forest growth and soil layer in Cunninghamia lanceolata plantations in mid-subtropical China. *Forest Ecology and Management*, **545**, 121302.
Wang Q Q, Xu H, Ma C B, Xue Y D, Wang C J, Xu M G, Zhang W J. 2018. Change of soil fertility and productivity of purple soil in Western China in recent 30 years. *Journal of Plant Nutrition and Fertilizers*, **24**, 1492–1499.
Wang T L, Wang G Y, Innes J L, Seely B, Chen B Z. 2017. ClimateAP: An application for dynamic local downscaling of historical and future climate data in Asia Pacific. *Frontiers of Agricultural Science and Engineering*, **4**, 448–458.
Wang X L, Wang A, Shi H H, Liu Z Y, Ma D M. 2014. Soil organic carbon density under different land use types on the Nanchangshan Island of Miaodao Archipelago. *Acta Scientiae Circumstantiae*, **34**, 1009–1015. (in Chinese)
Wen W, Peng Y G, Tan YF, Shi Z J. 2018. Characteristics of organic carbon distribution of major types of forest soils in Shenzhen. *Journal of Southwest Forestry University* (Natural Science), **38**, 106–113. (in Chinese)
Wiesmeier M, Spörlein P, Geuß U, Hangen E, Haug S, Reischl A, Schilling B, Lützow M V, Kögel-Knabner I. 2012. Soil organic carbon stocks in southeast Germany (Bavaria) as affected by land use, soil type and sampling depth. *Global Change Biology*, **18**, 2233–2245.
Xiao T, Ran F W, Li Z W, Wang S L, Nie X D, Liu Y J, Yang C R, Tan M, Feng S R. 2023. Sediment organic carbon dynamics response to land use change in diverse watershed anthropogenic activities. *Environment International*, **172**, 107788.
Xu Y N, Sheng J, Zhang L P, Sun G F, Zheng J C. 2025. Organic fertilizer substitution increased soil organic carbon through the association of microbial necromass C with iron oxides. *Soil and Tillage Research*, **248**, 106402.

Yang L, Jia W X, Shi Y, Zhang Z Y, Xiong H, Zhu G F. 2020. Spatiotemporal differentiation of soil organic carbon of grassland and its relationship with soil physicochemical properties on the northern slope of Qilian mountains, China. *Sustainability*, **12**, 9396.

Yang Y, Dou Y, Wang B, Wang Y, Liang C, An S, Soromotin A, Kuzyakov Y. 2022. Increasing contribution of microbial residues to soil organic carbon in grassland restoration chronosequence. *Soil Biology and Biochemistry*, **170**, 108688.

Yang Y H, Shi Y, Sun W J, Chang J F, Zhu J X, Chen L Y. Fang J Y. 2022. Terrestrial carbon sinks in China and around the world and their contribution to carbon neutrality. *Science in China* (Life Sciences), **52**, 534–574. (in Chinese)

Ye X H, Li J Q, Ma J H, Fan Q F, Yu N, Zhang Y L, Zou H T, Zhang Y L. 2023. Drip irrigation at a soil water suction of 30 kPa Helps AMF and GRSP to enhance greenhouse macro-aggregates. *Agronomy*, **13**, 522.

Yi T F, Xiang Y, Jiang J J, Peng L M. 2023. Determination of total boron in soil and deposit by inductively coupled plasma optical emission spectroscopy with four acids-microwave digestion. *Chinese Journal of Inorganic Analytical Chemistry*, **13**, 576–581. (in Chinese)

Yu M Z, Zhang L L, Xu X X, Feger K H, Wang Y H, Liu W Z, Schwaerzel K. 2015. Impact of land-use changes on soil hydraulic properties of Calcaric Regosols on the Loess Plateau, NW China. *Journal of Plant Nutrition and Soil Science*, **178**, 486–498.

Zenda T, Liu S T, Dong A Y, Duan H J. 2021. Revisiting sulphur-The once neglected nutrient: It's roles in plant growth, metabolism, stress tolerance and crop production. *Agriculture*, **11**, 626.

Zhou W, Wen S L, Zhang Y L, Gregory A S, Xu M G, Shah S A A, Zhang W J, Wu H H, Hartley I P. 2022. Long-term fertilization enhances soil carbon stability by increasing the ratio of passive carbon: Evidence from four typical croplands. *Plant and Soil*, **478**, 579–595.

Zhou Y, Wu W L, Meng F Q, Liu Y Y, Li H F. 2014. Review on the Content, Specification of Selenium and Its Availability in Soils. *Journal of Agricultural Resources and Environment*, **31**, 527–532.

Zhou Y C, Li D Y, Li Z L, Guo S B, Chen Z M, Wu L L, Zhao Y. 2023. Greenhouse gas emissions from soils amended with cornstalk biochar at different addition ratios. *International Journal of Environmental Research and Public Health*, **20**, 927.

Guest Editor Jinshui Wu
Managing Editor Lujuan Sun